Key controls on the seasonal and interannual variations of the carbonate system and air-sea CO_2 flux in the Northeast Atlantic (Bay of Biscay)

Zong-Pei Jiang,[1] David J. Hydes,[1] Toby Tyrrell,[1] Sue E. Hartman,[1] Mark C. Hartman,[1] Cynthia Dumousseaud,[1] Xose Antonio Padin,[2] Ingunn Skjelvan,[3] and César González-Pola[4]

Received 31 August 2012; revised 11 January 2013; accepted 16 January 2013; published 13 February 2013.

[1] Biogeochemical variations of surface water in the Northeast Atlantic (Bay of Biscay) were examined using high-frequency underway measurements combined with monthly sampling of carbon-related variables. The mechanisms controlling seasonal CO_2 variability were investigated by distinguishing the contributions of biological and physical processes to the monthly changes in dissolved inorganic carbon (DIC) and partial pressure of CO_2 (pCO_2). The seasonality of DIC (47–81 μmol kg^{-1}) had a single peak with a winter maximum primarily driven by vertical mixing and a summer minimum driven by spring biological removal. Non-Redfield C:N uptake was observed in the nutrient-depleted summer but not during the spring bloom. In the North Atlantic, pCO_2 seasonality shows a latitudinal transition: from the temperature-dominated oligotrophic subtropical gyre to the subpolar region where pCO_2 is dominated by changing concentrations of DIC. In the midlatitude Bay of Biscay, the annual cycle of pCO_2 (61–75 μatm) showed a double-peak distribution. The summer pCO_2 peak was mainly driven by temperature increase, while the winter peak resulted from the dominant effect of entrainment of subsurface water. Interannual variations of DIC were more pronounced in winter and were driven by the changes in the strength of winter mixing. Higher wintertime concentrations and seasonal amplitudes of DIC were observed in cold years when the mixed-layer depths were deeper, which appears to be associated with negative phases of the North Atlantic Oscillation. The Bay of Biscay shows a decrease of CO_2 uptake in 2008–2010 (−0.97 and −0.75 mol m^{-2} yr^{-1}) compared to 2002–2004 (−1.47 and −1.68 mol m^{-2} yr^{-1}).

Citation: Jiang, Z.-P., D. J. Hydes, T. Tyrrell, S. E. Hartman, M. C. Hartman, C. Dumousseaud, X. A. Padin, I. Skjelvan, and C. González-Pola (2013), Key controls on the seasonal and interannual variations of the carbonate system and air-sea CO_2 flux in the Northeast Atlantic (Bay of Biscay), *J. Geophys. Res. Oceans*, *118*, 785–800, doi:10.1002/jgrc.20087.

1. Introduction

[2] The ocean is an important sink taking up about a quarter of the anthropogenic CO_2 released each year [*Le Quere et al.*, 2009; *McKinley et al.*, 2011]. Oceanic carbon uptake slows the build-up of atmospheric CO_2 and mitigates human-driven climate change [*Fung et al.*, 2005; *Tyrrell*, 2011]. Meanwhile, the CO_2 invasion is acidifying the ocean and could have deleterious impacts on marine ecosystems [*Gattuso and Hansson*, 2011; *Orr et al.*, 2005]. There are large spatial and temporal variations in surface seawater biogeochemistry and air-sea CO_2 exchange across heterogeneous ocean regions [*Takahashi et al.*, 2009]. Knowledge of this spatiotemporal variability is critical in order to understand the current carbon cycle and to predict the future oceanic response to climate change.

[3] The North Atlantic is one of the strongest ocean sinks for natural and anthropogenic atmospheric CO_2 [*Sabine et al.*, 2004; *Takahashi et al.*, 2009; *Watson et al.*, 2009]. Much invaluable knowledge has been gained from the long-term measurements of carbon-related variables at marine time series stations in the North Atlantic, such as at BATS (Bermuda Atlantic Time-series Study) in the western North Atlantic subtropical gyre [*Bates*, 2001, 2007; *Bates et al.*, 1996], at ESTOC (European Station for Time Series in the ocean) in the eastern part of the North Atlantic subtropical gyre [*González-Dávila et al.*, 2003, 2007;

[1]National Oceanography Centre Southampton, University of Southampton, European Way, Southampton, UK.
[2]Instituto de Investigaciones Marinas, CSIC, Eduardo Cabello, Vigo, Spain.
[3]Bjerknes Center for Climate Research, Uni Research, Allegaten, Bergen, Norway.
[4]Instituto Español de Oceanografía, Centro Oceanográfico de Gijón, Gijón, Spain.

Corresponding author: Zong-Pei Jiang, National Oceanography Centre Southampton, University of Southampton, European Way, Southampton SO14 3ZH, UK. (zongpei.jiang@noc.soton.ac.uk)

2169-9275/13/10.1002/jgrc.20087

Santana-Casiano et al., 2007], and at OWSM (Ocean Weather Station M) in the Norwegian Sea [*Skjelvan et al*., 2008]. In recent years, acquisition of surface ocean CO_2 partial pressure (pCO_2) has been greatly expanded by the use of Ships of Opportunity (SOO, or Volunteer Observing Ship, VOS) equipped with underway measuring systems. Based on the observations obtained from time series stations and coordinated networks of SOO, several studies have tracked the changing CO_2 sink in the North Atlantic basin [*Corbiere et al*., 2007; *Schuster et al*., 2009; *Watson et al*., 2009]. These studies suggested substantial variations in the carbonate system and annual CO_2 fluxes on seasonal to decadal scales in the North Atlantic and also showed that interannual variability tends to be influenced by changes in large-scale climatic patterns.

[4] The Bay of Biscay is situated on the eastern side of the North Atlantic at midlatitudes; it is bounded by the Azores current from the subtropical gyre and the North Atlantic current from the subpolar gyre [*Lavin et al*., 2006]. The water masses of the Bay of Biscay mostly originate from the North Atlantic, and it is an area of deep winter mixing due to strong vertical convection [*Lavin et al*., 2006; *Pollard et al*., 1996]. Using data obtained from SOOs, *Padin et al*. [2008] examined the variability of oceanic CO_2 concentrations and CO_2 flux in the Bay of Biscay during 2002–2004. Based on an empirical algorithm developed from in situ observations, *Padin et al*. [2009] estimated the seawater pCO_2 from remotely sensed sea surface temperature (SST) and chlorophyll-*a* (Chl-*a*). However, most SOO measurements were limited to pCO_2 and basic ancillary environmental parameters such as temperature and salinity. Tracking the mechanisms controlling the variability of pCO_2 and CO_2 flux was difficult because of the lack of information on other important biogeochemical variables.

[5] To overcome this problem, monthly sampling of carbon-related variables in addition to high-frequency underway measurements were carried out since 2003 along the route of the MV *Pride of Bilbao* between Portsmouth (UK) and Bilbao (Spain) (http://www.noc.soton.ac.uk/ops/ferrybox_index.php) [*Hydes et al*., 2003, 2009]. This operation enabled some earlier studies of biogeochemical dynamics of surface waters on this route, particularly analyses of new production based on dissolved oxygen (DO) [*Bargeron et al*., 2006], variability of the carbonate system during 2005–2007 [*Dumousseaud et al*., 2010], and seasonal changes in the morphotypes of the coccolithophore *Emiliania huxleyi* [*Smith et al*., 2012].

[6] In this study, the records of two full annual cycles (SOO observations coupled with satellite data and subsurface data from Argo floats, September 2008 to September 2010) provide more details on the seasonal variations of the carbonate system, nutrients, and air-sea CO_2 flux in the Bay of Biscay. The mechanisms controlling seasonal carbon variability were investigated by separating the contributions of biological and physical processes to the monthly changes in dissolved inorganic carbon (DIC) and pCO_2. The data also allow us to follow the elemental stoichiometry of biological uptake of carbon and nutrients to evaluate the existence of "carbon overconsumption" [*Sambrotto et al*., 1993; *Toggweiler*, 1993] in the Northeast Atlantic. To examine the regional differences in seasonal patterns in the carbonate system in the North Atlantic, the data from the Bay of Biscay are compared to the time series observation results at BATS [*Bates*, 2001, 2007; *Bates et al*., 1996, http://bats.bios.edu/], ESTOC [*González-Dávila et al*., 2003, 2007; *Santana-Casiano et al*., 2007], and OWSM [*Skjelvan et al*., 2008]. Furthermore, trends in 2008–2010 are compared to those inferred from the 2005–2007 data along the same route [*Dumousseaud et al*., 2010] and the 2002–2004 data along an orthogonal route [*Padin et al*., 2008] (Figure 1). This extends the time series over which we can compare interannual variations to cover the years from 2002 to 2010. The interannual variability was investigated focusing on the role of winter mixing and its link with the large-scale climate variability such as the North Atlantic Oscillation (NAO) and the Eastern Atlantic pattern (EA).

2. Materials and Methods

2.1. Observations and Measurements

[7] The observational data in this study were obtained mainly from the MV *Pride of Bilbao*, which crossed various characteristic oceanographic regions from the English Channel to the Iberian Shelf [*Bargeron et al*., 2006]. Here we focus on the Bay of Biscay defined as latitudes 45–46.5°N along the ferry's route (Figure 1) where the riverine influence is relatively small. Starting in April 2002, high-resolution observations of SST, salinity, DO (since February 2005), and Chl-*a* florescence have been made continuously by an onboard "Ferrybox" system with an intake depth of 5 m below the surface [*Hydes et al*., 2003, 2009]. Discrete samples for DIC, total alkalinity (TA), nitrate plus nitrite (NO_x), silicate (DSi), phosphate (DIP), and coccolithophore abundance were collected monthly when possible from February 2005 onwards (nutrients from March 2003). The DIC and TA were

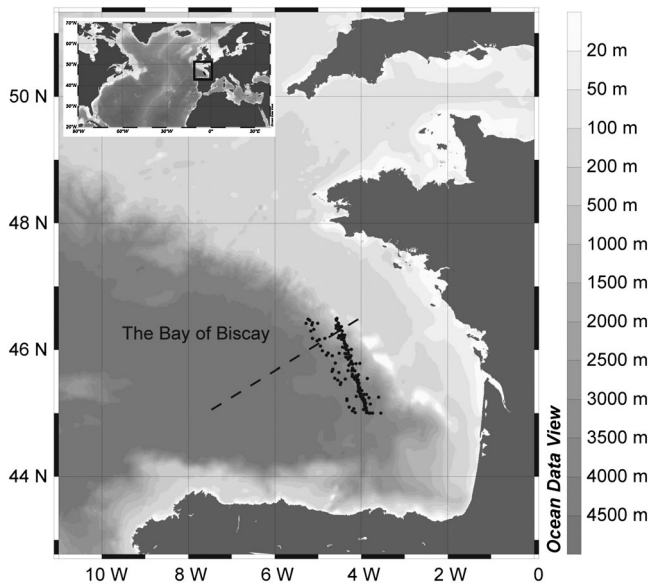

Figure 1. Map of the study region. The sampling positions of discrete samples in the Bay of Biscay are shown as dots (latitude 45–46.5°N along the route of MV *Pride of Bilbao*). The dashed line shows the route of underway CO_2 observations during 2002–2004 by *Padin et al*. [2008].

measured using the Marianda VINDTA 3C by coulometry and HCl titration, respectively [*Dickson et al*., 2007]. Nutrient samples were analyzed using standard methods [*Hansen and Koroleff*, 2007; *Hydes et al*., 2004]. Coccolithophore abundances were counted using scanning electron microscopy [*Smith et al*., 2012]. Details of these analytical methods were previously described by *Dumousseaud et al*. [2010] and are summarized in Table 1.

2.2. External Data

[8] A number of other data sources were used to develop our interpretation of the data from the MV *Pride of Bilbao*. Argo floats (http://www.coriolis.eu.org) provide temperature profiles in the Bay of Biscay for the estimation of the mixed-layer depth (MLD) following the fitting algorithm developed by *González-Pola et al*. [2007]. The monthly area-averaged Chl-*a* data (45–46°N, 5 – 3°W) from the 4 km global products of MODIS-Aqua (Giovanni online data system by the NASA GES DISC, http://reason.gsfc.nasa.gov/Giovanni/) provide a consistent indication of the phytoplankton biomass in the surface layer of the study region against which to compare the fluorescence measurements made on the ship. The atmospheric CO_2 measurements were obtained at three land stations (Mace Head: 53.33°N, 9.90°W, Ile Grande: 48.80°N, 3.58°W, and Pic du Midi: 42.94°N, 0.14°E) adjacent to our study region from the World Data Centre for Greenhouse Gases (http://gaw.kishou.go.jp/wdcgg/wdcgg.html). The in situ wind speed data came from the Gascogne Buoy moored in the Bay of Biscay (45.3°N, 5°W, UK's Met Office), and it was corrected to 10 m height assuming neutral stability [*Hoffman*, 2011]. The remotely measured wind speed data were collected from the QuikSCAT product provided by the Physical Oceanography Active Archive Center of the NASA Jet Propulsion Laboratory (http://poet.jpl.nasa.gov/).

2.3. Calculations

[9] *Salinity Normalization*: normalization to a constant salinity is commonly used to correct for the influence of freshwater addition and removal on the marine carbonate data:

$$nX = X/S_{\mathrm{obs}} \times S_{\mathrm{ref}} \tag{1}$$

where X is the measured variable (i.e., TA, DIC), S_{obs} is the measured salinity, and S_{ref} is the reference salinity (the mean observed value of 35.6 in our study). To account for the non-zero freshwater end member associated with the inputs of carbon and alkalinity from river, a region-specific term for $S = 0$ ($X^{S=0}$) was suggested to be used [*Cai et al*., 2010; *Friis et al*., 2003]:

$$nX = \left(X - X^{S=0}\right)/S_{\mathrm{obs}} \times S_{\mathrm{ref}} + X^{S=0} \tag{2}$$

[10] Although our study region is potentially affected by riverine freshwater, we used equation (1) to normalize DIC and TA because of the high uncertainties of the $X^{S=0}$ of the river end members and their changes in the estuary processes [*Abril et al*., 1999, 2003, 2004]. Suggested by the salinities of the discrete samples (Figure 2b) and the underway salinity measurements along the ship's route (Figure s1 in the supplement), using of equation (1) for salinity normalization is applicable during winter and spring when the riverine influence was minor. Although the signals of the riverine input were observed in summer months (Figure 2b and Figure s1), the uncertainty associated with the normalization did not significantly affect our discussion, as we only discussed the changes in DIC and pCO_2 during this period in a qualitative fashion (see section 4).

[11] *Carbonate Chemistry Calculation*: concentrations of different components of the carbonate system were calculated using the program "CO2SYS" [*Lewis and Wallace*, 1998] from the measured DIC, TA, and ancillary data. The carbonate and HSO_4^- dissociation constants were chosen as "*Mehrbach et al*., 1973 refitted by *Dickson and Millero*, 1987" [*Dickson and Millero*, 1987; *Mehrbach et al*., 1973] and "Dickson" [*Dickson*, 1990], respectively.

[12] *DO Anomaly*: The DO anomaly (DO_{anom}) was calculated as the difference between the measured DO

Table 1. Methodology and Accuracy of the Measured Variables

Variables	Type	Methodology	Accuracy
Sea surface temperature (SST)	underway	Aanderaa 4050 temperature sensor and SeaBird SBE48 hull temperature sensor	±0.05°C
Salinity	underway	Calculated from temperature (Aanderaa 4050 sensor) and conductivity (Aanderaa 3919 sensor), calibrated by the discrete samples measured by a Guildline Autosal salinometer (8400 B)	±0.03
Dissolved oxygen (DO)	underway	Aanaderaa 3930 sensor, calibrated by the discrete samples measured by onboard Winkler titration	±1 mmol m^{-3}
Dissolved inorganic carbon (DIC)	discrete	Coulometric titration by Marianda VINDTA 3C, corrected by Certified Reference Materials from Scripps Institution of Oceanography	±2 μmol kg^{-1}
Total alkalinity (TA)	discrete	HCl titration by Marianda VINDTA 3C, corrected by Certified Reference Materials from Scripps Institution of Oceanography	±2 μmol kg^{-1}
Nutrients	discrete	SEAL AutoAnalyzer	±0.1 μmol kg^{-1} for nitrate and nitrite; ±0.1 μmol kg^{-1} for silicate; ±0.02 μmol kg^{-1} for phosphate
Coccolithophore abundance	discrete	Scanning Electron Microscope (Carl Zeiss Leo 1450VP)	

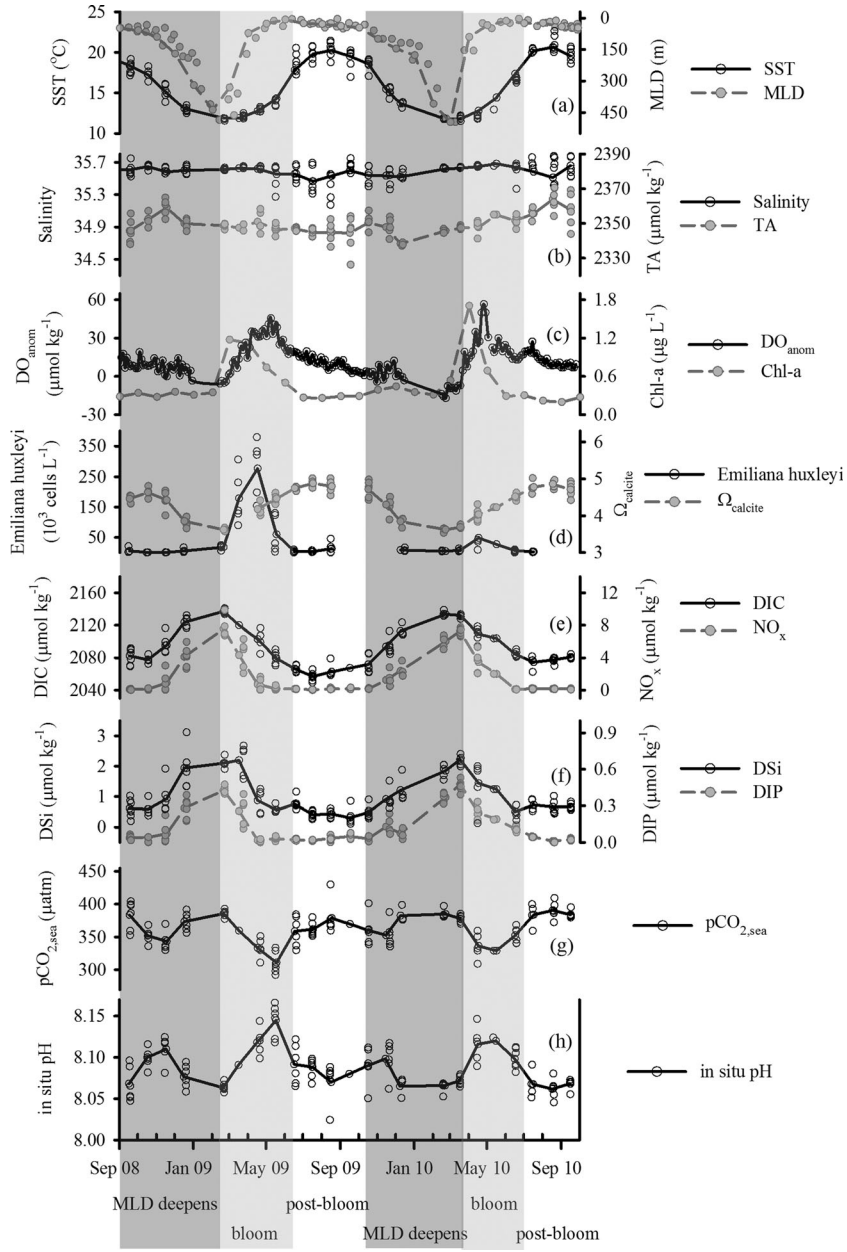

Figure 2. The biogeochemical variations of the surface water in the Bay of Biscay from September 2008 to September 2010: (a) SST and MLD, (b) salinity and TA, (c) DO_{anom} and remotely sensed Chl-*a* concentration, (d) DIC and NO_x, (e) *Emiliania huxleyi* cellular abundance and $\Omega_{calcite}$, (f) DSi and DIP, (g) pCO_2 calculated from DIC and TA, and (h) calculated in situ pH in total scale. The monthly averaged values were connected for a better visualization of the seasonal trend. The annual cycle was divided into three periods with different dominant controlling mechanism on DIC and pCO_2 variability (see the text for details).

concentration (DO_{obs}) and the saturated value (DO_{sat}) [*Benson and Krause*, 1984]:

$$DO_{anom} = DO_{obs} - DO_{sat} \quad (3)$$

[13] *Air-Sea Flux*: The air–sea flux of CO_2 (F_{CO2}) and O_2 (F_{O2}) were calculated as:

$$F_{CO2} = k_{(CO2)} \times \alpha \times \Delta pCO_{2,sea\text{-}air}, F_{O2} = k_{(O_2)} \times DO_{anom} \quad (4)$$

where α is the gas solubility of CO_2 as a function of seawater temperature and salinity [*Weiss*, 1974], $\Delta pCO_{2,sea\text{-}air}$ is the partial pressure difference of CO_2 between the seawater (calculated from the measured DIC and TA using "CO2SYS") and the atmosphere (measured by the adjacent land stations), and k is the gas transfer velocity which can be calculated from Schmidt number of CO_2 or O_2 and wind speed [*Wanninkhof*, 1992]. The wind speed data were obtained from in situ buoy measurement or remote sensing (QuikSCAT). In addition, three algorithms [*McGillis et al.*, 2001; *Nightingale et al.*, 2000; *Sweeney et al.*, 2007] were

used for calculation, and the results were compared to assess the uncertainty resulting from different parameterizations of the gas transfer velocity.

[14] *Contributions to the Monthly DIC Changes*: The observed changes in the concentration of salinity-normalized DIC ($\Delta nDIC_{obs}$) in the mixed-layer can be attributed to three groups of physical and biogeochemical processes-gas exchange (ΔDIC_{gas}), biological production (ΔDIC_{BP}), and mixing processes (ΔDIC_{mix}):

$$\Delta nDIC_{obs} = \Delta DIC_{gas} + \Delta DIC_{BP} + \Delta DIC_{mix} \quad (5)$$

[15] Since ΔDIC_{gas} and ΔDIC_{BP} can be estimated from the measurements but ΔDIC_{mix} is difficult to estimate directly, ΔDIC_{mix} was calculated by difference as:

$$\begin{aligned}\Delta DIC_{mix} &= \Delta nDIC_{obs} - \Delta DIC_{gas} - \Delta DIC_{BP} \\ &= \Delta nDIC_{obs} - F_{CO2}/MLD - NCP_{MLD}/MLD \end{aligned} \quad (6)$$

where ΔDIC_{gas} is estimated from the air-sea CO_2 flux and MLD and NCP_{MLD} is the MLD-integrated net community production (NCP). For the biological term ΔDIC_{BP}, we only considered the effect of NCP but ignored the influence of calcification because of the relatively low coccolithophore abundance [*Smith et al.*, 2012]. NCP_{MLD} can be estimated from the changes in the concentrations of NO_x, DIC, or DO. The frequency of DO measurements (1–3 days at a given position) have better temporal resolution than those of NO_x and DIC (monthly) in this study. Therefore, NCP_{MLD} was calculated from the changes in the gas transfer–corrected DO_{anom} ($DO_{anom}{}^{GasCorr}$):

$$DO_{anom}{}^{GasCorr} = DO_{anom} + \Delta DO_{gas} = DO_{anom} + F_{O2}/MLD \quad (7)$$

where the DO_{anom} is corrected for the effect of gas exchange (ΔDO_{gas}). Considering the relative quick equilibration time of oxygen, the monthly air-sea O_2 flux (F_{O2}) was calculated as the mean value of the 3-day fluxes. NCP_{MLD} was then estimated as:

$$\begin{aligned}NCP_{MLD} = &\left(DO_{anom}{}^{GasCorr}{}_{m+1} - DO_{anom}{}^{GasCorr}{}_{m}\right) \\ &\times (MLD_{m+1} + MLD_m)/2 \times (C:O)_{NCP}\end{aligned} \quad (8)$$

where $(DO_{anom}{}^{GasCorr}{}_{m+1} - DO_{anom}{}^{GasCorr}{}_{m})$ is the difference in $DO_{anom}{}^{GasCorr}$ between two consecutive months, $(MLD_{m+1} + MLD_m)$ / 2 is the average MLD in those 2 months, and the Redfield $(C:O)_{NCP}$ ratio of 106:138 was used to convert the changes in oxygen to those of carbon.

[16] During the spring bloom, the effect of entrainment was insignificant (shoaling of MLD) and the riverine influence was also minor (relatively constant salinity, Figure 2b). Therefore, our estimates of NCP_{MLD} during spring were little affected by the mixing effects. During autumn and winter with a deepening MLD, equation (8) underestimated the NCP_{MLD} since it did not account for the portion of production that balances the DO decrease induced by convection. However, this did not affect our ability to identify the major controlling factor of DIC variations (see section 4.1). In the stratified conditions from May to September/October, changes in concentrations of DIC are sensitive to small changes in biological or physical processes (including the riverine influence) acting on the small volume of water above the summer thermocline. Consequently, we did not separate the biological and mixing effects in this period and their combined effect was presented instead (ΔDIC_{BP+mix} in Figure 5a).

[17] *Temperature Effect on pCO_2*: The thermally forced pCO_2 variation ($pCO_{2,Temp}$) was calculated under isochemical conditions (DIC and TA fixed at their mean values of 2093 and 2350 $\mu mol\,kg^{-1}$, respectively) but with CO_2 solubility varying as a function of the measured temperature. Additionally, the temperature-normalized pCO_2 ($pCO_{2,NT}$) was calculated from the measured DIC and TA at the mean temperature (16.0 °C).

[18] *Contributions to the Monthly Changes in pCO_2*: Seawater pCO_2 is mainly a function of temperature, DIC, TA, and salinity [*Takahashi et al.*, 1993]. All the processes affecting DIC in equation (5) would result in corresponding changes in pCO_2, and pCO_2 is further modulated by the changes in TA and temperature. In a similar way to equation (5), we broke down the monthly variability of the calculated pCO_2 into the contributions of different biological and physical processes:

$$\begin{aligned}\Delta pCO_2 = &\Delta pCO_{2,(\Delta DICgas)} \\ &+\Delta pCO_{2,(\Delta DIC_{BP})} + \Delta pCO_{2,(\Delta DICmix)} \\ &+\Delta pCO_{2,(\Delta TAmix)} + \Delta pCO_{2,(\Delta Temp)}\end{aligned} \quad (10)$$

where the subscripts of ΔpCO_2 correspond to the factors controlling variations in pCO_2 resulting from the changes in DIC (ΔDIC_{gas}, ΔDIC_{BP}, ΔDIC_{mix}), TA (ΔTA_{mix}), and temperature ($\Delta Temp$). ΔDIC_{gas}, ΔDIC_{BP}, and ΔDIC_{mix} were estimated from the equation (5). ΔTA_{mix} was calculated from changes in the observed TA which were corrected for the uptake or release of nutrients according to the nutrient-H^+-compensation principle [*Wolf-Gladrow et al.*, 2007]. $\Delta Temp$ was calculated from the observed temperature changes.

[19] Each term in equation (10) was calculated on a monthly basis assuming that each process acted on the seawater carbonate system individually. The changes in DIC, TA, and temperature caused by each process were considered in turn while the other variables were held constant. The difference in pCO_2 between the original state and the modified conditions were then calculated. Uncertainties of the calculations of equations (5) and (10) were estimated from the errors of measurements (Table 1) and as was their propagation through the calculations [*Taylor*, 1982].

3. Seasonal Variations

[20] The plots in Figure 2 show the seasonal cycles in the Bay of Biscay covering the two full annual cycles between September 2008 and September 2010.

3.1. Hydrography and Environmental Variables

[21] The seasonal amplitudes of the monthly mean SST (Figure 2a) were 8.4 °C and 8.9 °C in the 2 years, respectively. Winter minima in SST occurred in February 2009 (11.9 °C) and March 2010 (11.8 °C), and summer maxima occurred in August in both years (20.3 °C and 20.6 °C). The seasonal evolution of MLD was coupled to the changes in SST (Figure 2a). The deepening of the MLD progressed from autumn along with decreasing SST and developed to 400–500 m in the coldest months. A transition from deep winter mixing to shallow stratification was observed in spring, and stable stratification (~20 m) developed in May and then remained throughout the summer. The monthly mean salinity ranged from 35.46 to 35.68 without an obvious seasonal trend, but most low salinities were observed during the post-bloom summer months (Figure 2b and Figure s1 in the supplement). The low salinity surface water along this SOO route and its movement relating to the wind and current was discussed by *Kelly-Gerreyn et al*. [2006].

[22] The remotely sensed Chl-*a* (Figure 2c) peaked during the spring blooms (up to 1.2 and 1.7 mg m^{-3} in 2009 and 2010, respectively) compared to the low concentrations in other seasons (~0.3 mg m^{-3}). Coccolithophore abundance showed a similar pattern to that of Chl-*a* (Figures 2c, 2d). The concentration of the dominant species of coccolithophores (*Emiliana huxleyi*) peaked in April (2.77×10^5 and 0.46×10^5 cells L^{-1} in 2009 and 2010, respectively) but well below bloom levels (10^6 cells L^{-1}). Together with the increasing phytoplankton biomass, DO_{anom} increased during spring reaching 33.4 μmol kg^{-1} in May 2009 and 35.5 μmol kg^{-1} in April 2010. It then decreased toward winter to a slight undersaturation in February (Figure 2c).

3.2. Carbonate System and Nutrients

[23] The ranges of the monthly averaged TA were 15 and 26 μmol kg^{-1} in 2008/2009 and 2009/2010, respectively, but there was not a clear seasonal trend in TA variations (Figure 2b). Salinity normalization ($nTA_{35.6}$ in Figure 3b) did not explain the TA variations. The local calcification influence on TA was expected to be minor because of the low abundance of coccolithophores (Figure 2d). The small difference between $nTA_{35.6}$ and the potential TA ($pTA = nTA + NO_x$) in Figure 3b indicated that uptake or release of nutrients during the organic production also did not have a significant influence on the TA variability. Therefore, mixing processes (i.e., riverine influence or advection of water mass with calcification signals) appear to be more important than the local biological processes affecting the TA concentration in our study region. The measured values of TA were generally higher than those predicted using a published algorithm for the north Atlantic open ocean based on SST and salinity (TA_{Lee} in Figure 3a) [*Lee et al*., 2006]. This suggests additional TA sources to our study region, which may be related to the high TA concentrations of the rivers Loire and Gironde and the addition of TA in the estuary [*Abril et al*., 1999, 2003, 2004].

[24] In contrast, DIC showed a clear seasonality (Figure 2e) that varied inversely with SST and MLD (Figure 2a). The concentrations of DIC increased in autumn and winter, at a time when there was decreasing SST and deepening of the MLD. The annual maximum concentrations of DIC in February (2137 μmol kg^{-1} in 2009 and 2134 μmol kg^{-1} in 2010) were followed by decreases through spring to summer minima in July (2057 μmol kg^{-1} in 2009 and 2072 μmol kg^{-1} in 2010) (Figure 2e). Figure 2d presents the calculated saturation state of the calcite form of $CaCO_3$ (Ω): $\Omega_{calcite} = [Ca^{2+}] \times [CO_3^{2-}]/K'_{sp(calcite)}$, where $[Ca^{2+}]$ and $[CO_3^{2-}]$ are the concentrations of Ca^{2+} and CO_3^{2-}, and $K'_{sp(calcite)}$ is the stoichiometric solubility product of calcite. Higher values of Ω favor the formation of $CaCO_3$ shells and skeleton, while values lower than 1 are corrosive to $CaCO_3$ [*Feely et al*., 2008]. The $\Omega_{calcite}$ was constantly above 1 in our study region, and its seasonal cycle was opposite to that of DIC with higher values in summer (~5.2) and lower values in winter (~3.6). The potential effects of these changes on coccolithophores have been considered in the associated study of *Smith et al*. [2012].

[25] Similar to DIC, concentrations of nutrients (Figures 2e, 2f) increased from autumn to maxima in late winter (7.6 and 7.3 μmol kg^{-1} for NO_x, 0.43 and 0.48 μmol kg^{-1} for DIP, 2.20 and 2.22 μmol kg^{-1} for DSi in 2008/2009 and 2009/2010, respectively). During spring, nutrients showed parallel declines associated with DIC drawdown and corresponding increases in Chl-*a* and DO_{anom} (Figure 2). Concentrations of NO_x and DIP decreased to a depleted level at the onset of stratification and remained low throughout the summer (<0.15 μmol kg^{-1} for NO_x and <0.05 μmol kg^{-1} for DIP, respectively), while the concentrations of DSi remained at ~0.5 μmol kg^{-1} in the summer (Figures 2e, 2f).

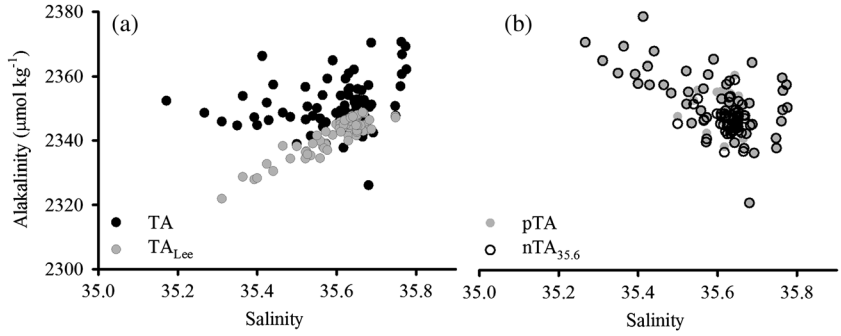

Figure 3. Alkalinity versus salinity: (a) measured TA and TA_{Lee} predicted from SST and salinity using *Lee et al.'s* [2006] algorism and (b) TA normalized to the mean salinity of 35.6 ($nTA_{35.6}$) and potential TA ($pTA = TA + NO_x$).

[26] In contrast to the single annual peak in DIC, the calculated seawater pCO_2 was characterized by a double-peak annual cycle (Figure 2 g). One peak in pCO_2 was observed in the late winter (386 and 385 µatm in February 2009 and 2010, respectively) together with the annual maxima of DIC and nutrients, while the second peak in summer (379 and 390 µatm in August 2009 and 2010, respectively) corresponded to the annual maximum SST. The corresponding two minima in pCO_2 were observed in early winter (337 and 346 µatm in November 2009 and 2010, respectively) and late spring (311 and 329 µatm in May 2009 and 2010, respectively). The calculated in situ pH ranged from 8.02 to 8.17, showing a mirror image of the distribution of pCO_2 (Figure 2 h).

3.3. Air-Sea CO_2 Flux

[27] The air-sea CO_2 exchange is driven by the pCO_2 differences across the air-sea interface ($\Delta pCO_{2,sea\text{-}air}$ in Figure 4a). The atmospheric pCO_2 showed a seasonal variability of ~16 µatm in 2008–2010 (not shown), which is lower than that in the seawater (75 and 61 µatm, Figure 2 g). Therefore, $\Delta pCO_{2,sea\text{-}air}$ were determined more by the greater variations in the seawater $pCO_{2,sea}$. Figure 4a shows that surface seawater in the Bay of Biscay was undersaturated in pCO_2 in autumn (October to November) and spring (March to June) in both years. In contrast, pCO_2 in seawater was close to equilibrium with the atmosphere in winter (December to February) and became slightly supersaturated in CO_2 in summer (July to September). The second factor determining the rate of CO_2 exchange is wind speed [*Wanninkhof*, 1992]. Over the Bay of Biscay, winds tend to be governed by the Azores High and Iceland Low [*Lavin et al*., 2006]. The wind speeds measured at the Gascogne Buoy had similar patterns in both years (Figure 4b): higher in winter and weaker in spring and summer. The QuikSCAT wind speeds showed similar trends when compared to the buoy measurements and were ~0.5 m s^{-1} lower than the in situ wind speed.

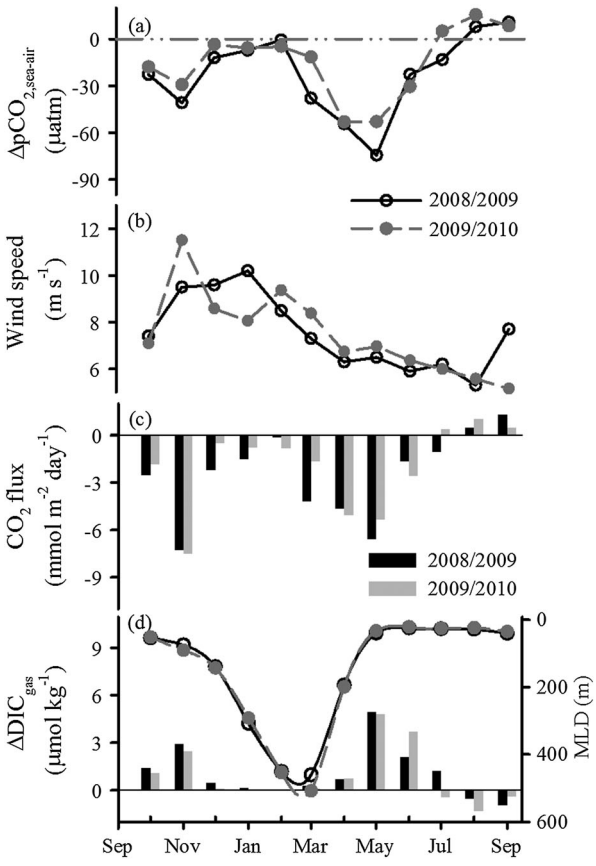

Figure 4. (a) pCO_2 difference between surface seawater and atmosphere ($\Delta pCO_{2,sea\text{–}air}$); (b) in situ wind speed by buoy measurement; (c) air-sea CO_2 flux calculated using in situ wind speed and parameterization following *Nightingale et al*. [2000]—the negative fluxes refer to the gas transfer from atmoshphere to sea; (d) MLD and gas exchange-induced changes in DIC (ΔDIC_{gas}).

[28] Due to the similarity of the patterns in variation of $\Delta pCO_{2,sea\text{-}air}$ and wind speed between years, the air-sea CO_2 flux seasonal patterns were also similar in 2008/2009 and 2009/2010 (Figure 4c). Two periods of greater oceanic CO_2 uptakes were observed: at the end of spring bloom and at the onset of winter turnover. The former period was mainly associated with more negative $\Delta pCO_{2,sea\text{-}air}$ and the other with high wind speed. The Bay of Biscay became neutral or turned into a weak CO_2 source to the atmosphere at the times of the two peaks in $\Delta pCO_{2,sea}$ toward the end of winter and in summer (Figure 4c).

[29] The annual CO_2 flux was integrated from the monthly fluxes. The three algorithms of gas transfer calculation [*McGillis et al*., 2001; *Nightingale et al*., 2000; *Sweeney et al*., 2007] and the two sets of wind speed data (in situ buoy measurement and remotely QuikSCAT data) were used to estimate the uncertainty for the CO_2 flux estimation (Table 2). When the in situ wind speed was used, the annual CO_2 fluxes calculated following the three algorithms were -1.05 ± 0.04 and -0.88 ± 0.06 mol m^{-2} yr^{-1} in 2008/2009 and 2009/2010, respectively. The annual fluxes estimated from the QuikSCAT data were -1.01 ± 0.03 mol m^{-2} yr^{-1} in 2008/2009 and -0.81 ± 0.05 mol m^{-2} yr^{-1} in 2009/2010 (gaps in the QuikSCAT record in 2009/2010 were filled by estimation based on the in situ measurements and their correlation with QuikSCAT data during 2005–2009, $R^2 = 0.89$).

[30] Figure 4d shows the gas transfer-induced DIC changes and their relationship with the air-sea CO_2 flux and MLD. It suggests that gas exchange had little influence on changing concentrations of DIC between December and April as the CO_2 influx from gas exchange was diluted into

Table 2. The Annual CO_2 Fux (mol m^{-2} yr^{-1}) Calculated from Different Wind Speeds and Parameterizations of Gas Transfer Velocity[a]

Wind speed Parameterization	QuikSCAT			Buoy measurement		
	N00	M01	S07	N00	M01	S07
2002/2003	–1.47	–1.60	–1.59			
2003/2004	–1.68	–1.80	–1.81			
2008/2009	–0.97	–1.02	–1.04	–1.01	–1.05	–1.08
2009/2010	–0.75	–0.85	–0.82	–0.82	–0.94	–0.89

[a]The wind speed data were from QuikSCAT remote sensing and in situ buoy measurements (no available data in 2002–2004). Three parameterizations of the gas transfer welocity were used: *McGillis et al*. [2001] (M01), *Nightingale et al*. [2000] (N00), *Sweeney et al*. [2007] (S07).

a large volume of water as the mixed-layer was relatively deep. In contrast, CO_2 invasion from the atmosphere noticeably increased concentrations of DIC in the post-bloom period (May to July) and autumn (October and November). These were times of a high air-sea CO_2 flux entering a shallow mixed-layer.

4. Controlling Mechanisms of the Seasonal Variations of DIC and pCO_2

[31] To better examine the seasonal variability, we divided the annual cycle into three periods (Figures 2 and 5). This is similar to the division in "pre-bloom, bloom, and post-bloom" periods made by *Padin et al.* [2008] but is here based on the evolution of MLD and concentrations of nutrients. The first period "MLD deepens" covers autumn and winter with the progressive deepening of the MLD (October to February/March). The second period "spring bloom" is from the month with the maximum nutrient concentrations to when nutrients were depleted (February/March to May). The third period "post-bloom" is summer with surface stratification from June to September. In Figure 5, monthly changes in DIC and pCO_2 were partitioned into the contribution from the individual biological and physical controlling factors using equations (5) and (10).

4.1. Key Controls on the Seasonality of DIC

[32] During the period of "MLD deepens," concentrations of DIC showed an increasing trend along with the deepening of the MLD (Figure 2). As DIC increases with depth (Figure s2 in the supplement), the entrainment of deep water enriched in CO_2 elevated the concentration of DIC in the surface layer. As shown in Figure 5a, the net increases in DIC during this period mainly resulted from the effect of mixing processes (ΔDIC_{mix}), which overcame the influences of biological activities (ΔDIC_{BP}) and gas transfer (ΔDIC_{gas}). If a well-mixed state of the upper 470 m (the maximum MLD in the two winters) water column was assumed, the DIC concentration (2132 $\mu mol\,kg^{-1}$) calculated from the vertical profiles (measured in September 2005, Figure s2 in the supplement) corresponded well with the observed winter peaks (2137 and 2134 $\mu mol\,kg^{-1}$ in 2009 and 2010 in Figure 2e). Therefore, the convection-induced DIC increase was the major driver of the increasing DIC concentration in the "MLD deepens" period.

[33] During the "spring bloom" period, concentrations of Chl-*a* increased significantly fueled by the nutrients supplied from the preceding winter mixing (Figure 2). The autotrophic biological production (ΔDIC_{BP} in Figure 5a) resulted in declines in DIC and nutrients (Figures 2e, 2f) accompanied by the production of DO (Figure 2c). Meanwhile, the mixing effect (ΔDIC_{mix} in Figure 5a) is small as the MLD is shoaling. Photosynthetic uptake was thus the dominant process resulting in the drawdown of DIC and nutrients in the productive "spring bloom" period.

[34] The mixed-layer during the "post-bloom" period was characterized by depleted nutrients and strong stratification, and the concentration of DIC was unusually prone to change because of the shallow MLD. During this period, biological production was limited by nutrient scarcity; vertical mixing was suppressed by stratification; but the salinity data suggested the influence of river water (Figure 2b). DIC variability in the "post-bloom" period was controlled by a combination of biological and physical effects without a single dominant controlling factor. Therefore, the effects of biological and mixing were not separated in this period and their combined effect was presented (ΔDIC_{BP+mix} in Figure 5a).

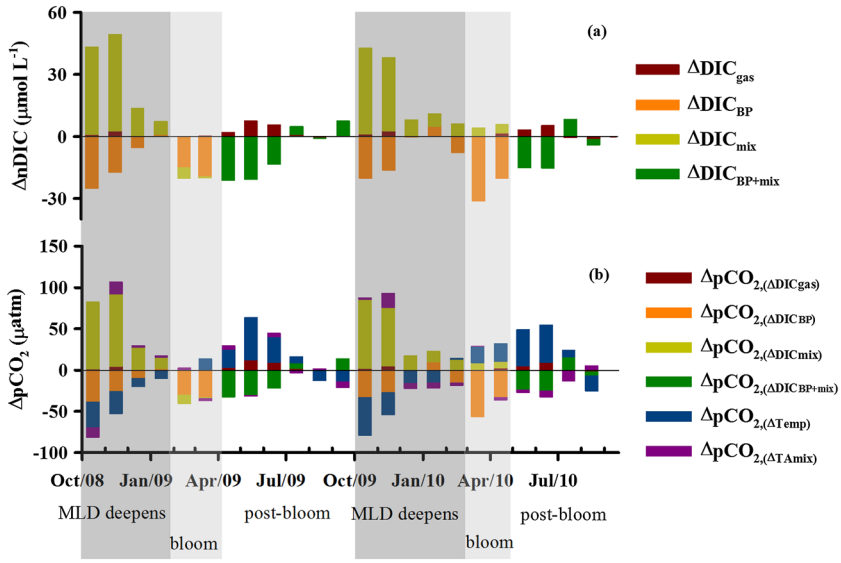

Figure 5. (a) Contributions to monthly changes in the salinity-normalized DIC (ΔDIC) from individual processes as indicated by the subscripts: gas exchange ("gas"), mixing ("mix"), biological production ("BP"). The biological and mixing influence were not separated during the stratified post-bloom period and their combined effect ("BP + mix") was shown. (b) The corresponding changes in pCO_2 resulted from these changes in DIC were presented together with those resulted from the changes in temperature ($\Delta pCO_{2,(\Delta Temp)}$) and mixing-induced TA changes ($\Delta pCO_{2,(\Delta TAmix)}$). See the text for details.

4.2. Key Controls on the Seasonality of pCO_2

[35] The seasonal ranges in SST in the Bay of Biscay resulted in corresponding thermally driven pCO_2 variations ($pCO_{2,Temp}$ in Figure 6a) of 126 and 136 µatm in 2008/2009 and 2009/2010, respectively. On the other hand, the temperature-normalized $pCO_{2,NT}$ (Figure 6a) reflects the influence of nonthermal processes (i.e., air-sea CO_2 transfer, biological activity, and mixing) on pCO_2 variability [*Körtzinger et al.*, 2008]. $pCO_{2,NT}$ displays an annual cycle similar to the concentration changes in DIC (Figure 2e), and its seasonal amplitudes were 154 and 143 µatm in 2008/2009 and 2009/2010, respectively (Figure 6a). The opposite trend between $pCO_{2,Temp}$ and $pCO_{2,NT}$ (Figure 6a) suggests a competing effect of temperature and the nonthermal processes on the pCO_2 variability. Figure 6a also shows that temperature was the dominant driver of changes in pCO_2 in summer ($pCO_{2,Temp} > pCO_{2,NT}$) while the nonthermal forcing of pCO_2 exceeded the temperature effect in other seasons ($pCO_{2,Temp} < pCO_{2,NT}$).

[36] Considering the contributions of the various processes to the monthly changes in pCO_2 (equation 10), the result shown in Figure 5b suggests that the influence of temperature ($\Delta pCO_{2,(\Delta Temp)}$), biological production ($\Delta pCO_{2,(\Delta DIC_{BP})}$), and mixing-induced changes in DIC ($\Delta pCO_{2,(\Delta DICmix)}$) were more important than gas transfer ($\Delta pCO_{2,(\Delta DICgas)}$) and mixing-induced changes in TA ($\Delta pCO_{2,(\Delta TAmix)}$) throughout the annual cycle. During the "MLD deepens" period, $\Delta pCO_{2,(\Delta DICmix)}$ was the dominant driver of the pCO_2 increases (Figure 5b). The entrainment of the CO_2-rich subsurface water led to a net increase in pCO_2 overriding the pCO_2 decreases resulting from the seasonal cooling ($\Delta pCO_{2,(\Delta Temp)}$) and biological $\Delta pCO_{2,(\Delta DIC_{BP})}$. During the "spring bloom" period, pCO_2 drawdown was mostly explained by the photosynthetic uptake of $\Delta pCO_{2,BP}$, which exceeded the increasing tendency due to surface warming (Figure 5b). From autumn to spring, the major controlling factors on pCO_2 were the same as those acting on concentrations of DIC; therefore, pCO_2 varied in phase with DIC during these periods (Figures 2e, 2 g). However, the $\Delta pCO_{2,(\Delta Temp)}$ and CO_2 invasion ($\Delta pCO_{2,(\Delta DICgas)}$) exceeded the combined effects of biological production and mixing ($\Delta pCO_{2,(\Delta DIC_{BP}+mix)}$) during the stratified summer conditions (Figure 5b). The dominance of the temperature effect over other nonthermal processes resulted in the summer pCO_2 peak occurring at the same time as the highest SST.

[37] The key controls on the double-peak distribution of the pCO_2 annual cycle were also shown by the relationship between pCO_2 and NO_x (Figures 6b, 6c). The peaks of pCO_2 and NO_x (as well as DIC) in late winter were mainly generated by convection-driven winter increases and biological-induced spring decreases. In contrast, low biological production in the nutrient-depleted surface seawater during the stratified "post-bloom" period results in temperature becoming the dominant control on the pCO_2 variations in summer.

5. C:N Stoichiometry

[38] The Redfield stoichiometry [*Redfield et al.*, 1934] is a basic paradigm in ocean biogeochemistry relating the fluxes of carbon and nutrients through the production and remineralization cycle. Recent studies have suggested that the stoichiometry of NCP may differ from the Redfield ratio. "Carbon overconsumption," i.e., the elevated consumption of carbon relative to the Redfield equivalent of nutrient uptake (C:N = 6.6), has been reported for the surface ocean including the North Atlantic [*Sambrotto et al.*, 1993; *Toggweiler*, 1993]. The C:N ratio of NCP, $(C:N)_{NCP}$,

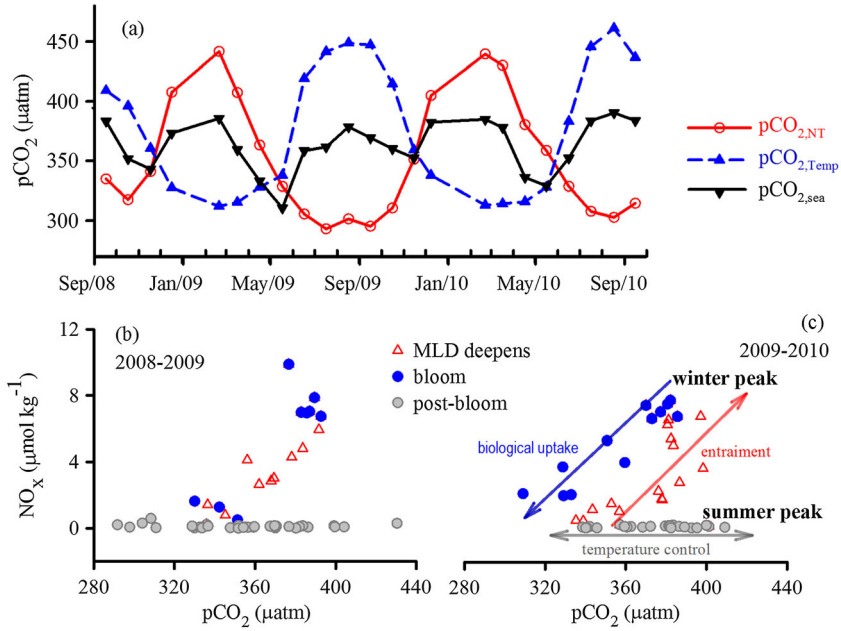

Figure 6. (a) The monthly averaged seawater $pCO_{2,sea}$, temperature-normalized $pCO_{2,NT}$, and thermally driven pCO_2 variations ($pCO_{2,Temp}$). The variations of NO_x and pCO_2 in 2008–2009 (b) and 2009–2010 (c); the major controls resulting in the summer and winter peaks in pCO_2 were showed in Figure 6c.

estimated from the mixed-layer regression of DIC and nitrate in the 1989 North Atlantic Bloom Experiment (NABE) was well above the Redfield value (up to 14.2 ± 0.2 [*Sambrotto et al.*, 1993]). Along an Atlantic transect (30–60°N, 20°W) covering different trophic states with migrating spring bloom conditions, *Körtzinger et al.* [2001] reported an increasing $(C:N)_{NCP}$ from pre- or early bloom condition (5–6) to the post-bloom/oligotrophic system (10–16). At a single point, the $(C:N)_{NCP}$ estimated from observations of pCO_2 and nitrate on a mooring (49°N, 16.5°W) was 11.0 ± 0.7 [*Körtzinger et al.*, 2008]. On a basin-integrated scale in the North Atlantic (40–65°N), the C:N ratio of new production estimated from climatological data (11.4 ± 1.4) also far exceeds the Redfield value [*Koeve*, 2006]. However, a reanalysis of the NABE data and the 20°W transect data [*Koeve*, 2004] suggested that the average seasonally integrated cumulative $(C:N)_{NCP}$ between winter mixing and the end of bloom is not significantly different from the Redfield ratio. *Koeve* [2004] also suggested that the elevated $(C:N)_{NCP}$ in the temperate and subarctic Northeast Atlantic was probably generated from carbon overconsumption in summer rather than during spring bloom.

[39] The NABE data are only from observations over a 2-week period [*Sambrotto et al.*, 1993], and extrapolation from spatial patterns along the 20°W transect to a model for seasonal progression [*Körtzinger et al.*, 2001] is open to question. *Koeve* [2004] also pointed out that the estimations of $(C:N)_{NCP}$ critically depend on determination of the preformed winter DIC and nutrient concentrations. In this study, we directly observed the wintertime concentrations of DIC and nutrients and the subsequent changes in their concentrations month by month. This enables a reliable and direct evaluation of the progression of elemental stoichiometry of $(C:N:P)_{NCP}$.

[40] To accurately estimate the $(C:N:P)_{NCP}$, the salinity-normalized DIC concentrations were corrected for the air-sea exchange ($nDIC^{GasCorr}$, Figures 7a, 7b) to account for the biasing effect of gas exchange. The effect of calcification was neglectable on the basis of the low coccolithophores abundance and the small TA variability as discussed above. The relative changes in $nDIC^{GasCorr}$, NO_x and DIP during the three periods are shown in Figure 7. The slopes estimated from linear regression during the spring bloom period reflect the time integrated uptake ratios of DIC and nutrients. The samples with NO_x concentrations lower than $0.5\ \mu mol\ kg^{-1}$ were discarded in the regression to avoid the effect of nutrient limitation [*Sambrotto et al.*, 1993].

[41] The ratios of $(C:N)_{NCP}$ were 5.77 ± 0.45 ($R^2 = 0.96$) and 6.56 ± 0.71 ($R^2 = 0.89$) in the 2 years (Figures 7a, 7b), respectively. These values did not show "carbon overconsumption" during the spring bloom when nutrients were not limiting. However, closer inspection shows that DIC continued to decrease after the end of bloom when NO_x was undetectable (Figures 2, 7a, 7b). So we appear to be seeing non-Redfield consumption of carbon versus nitrogen in the "post-bloom" period with nutrient stress. This may possibly be attributed to the riverine influence, or preferential recycling of nutrients [*Bozec et al.*, 2006; *Koeve*, 2006] or other potential nutrient inputs such as nitrogen fixation [*Chou et al.*, 2006; *Rees et al.*, 2009] and the short-lived transportation of nitrate from deep stocks [*Johnson et al.*, 2010].

[42] Our observations confirm *Koeve's* [2004] suggestion that apparent overconsumption of carbon relative to nitrogen occurs after the spring bloom in the Northeast Atlantic.

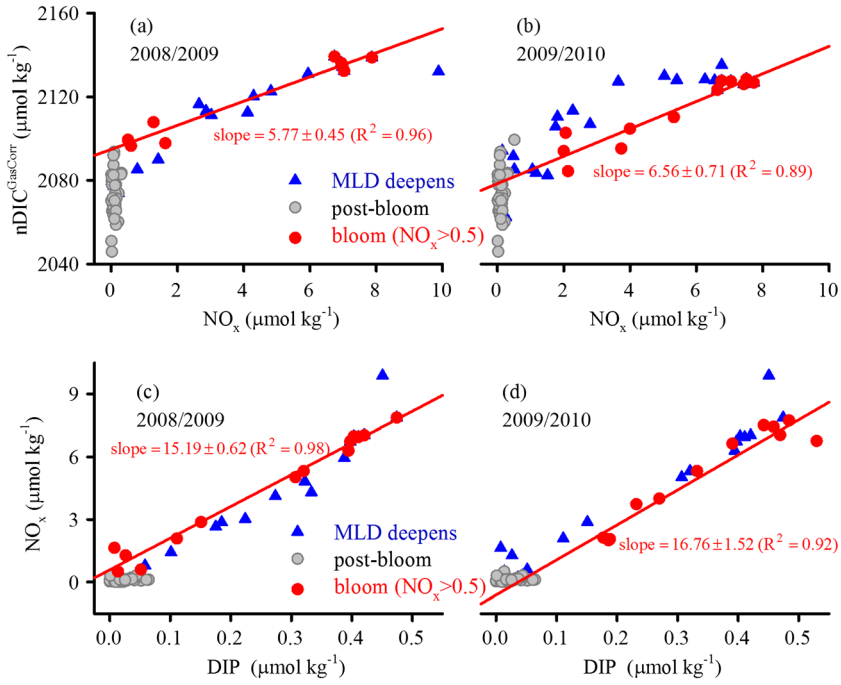

Figure 7. The concentrations of salinity-normalized DIC corrected for gas exchange ($nDIC^{GasCorr}$) and NO_x in different periods in year 2008–2009 (a) and 2009–2010 (b); the concentrations of NO_x and DIP in different periods in year 2008–2009 (c) and 2009–2010 (d). The regressions were based on data collected during the spring bloom period with NO_x concentration higher than $0.5\ \mu mol\ kg^{-1}$.

Moreover, $(C:N)_{NCP}$ ratio in our study would have been overestimated if it had been calculated simply based on DIC and NO_x at two timepoints, which included the "post-bloom" period. This demonstrates that care needs to be taken when using sparse data sets to infer discrepancies relative to the Refield ratio. Meanwhile, the $(N:P)_{NCP}$ in the 2 years (15.19 ± 0.62 and 16.76 ± 1.52; Figures 7c, 7d) was not significantly different from the classic Redfield ratio value of 16, apparently contrary to the suggestions that "bloom-formers" should have low N:P ratio (≤10) [*Klausmeier et al.*, 2004; *Quigg et al.*, 2003].

6. Comparison of the Seasonal Carbon Variability in the North Atlantic

[43] In Figure 8 and Table 3, the seasonal variations of SST, DIC, and pCO_2 in the Bay of Biscay are compared to other time series observations in the North Atlantic from the subtropical gyre (BATS, ESTOC) and from the subpolar region (OWSM). The SST is lower at high latitudes and shows a similar seasonal pattern at all three locations in the North Atlantic (Figure 8a). In all areas, the seasonality of DIC is similarly characterized by winter-spring maxima associated primarily with entrainment of subsurface water and summer-autumn minima generated from biological uptake. The DIC concentrations at OWSM and in the Bay of Biscay were generally higher than those at BATS especially during the winter (Figure 8b). This mainly resulted from the higher CO_2 solubility (due to the lower SST) and the stronger intensity of winter mixing at higher latitudes. Winter maxima in nutrients also have higher values in the high latitude regions (Table 3) because of the stronger winter convection. As a result of higher winter-preformed concentrations of DIC and stronger biological removal stimulated by the higher winter upward nutrient supply, the seasonal amplitudes of DIC at OWSM and in the Bay of Biscay were higher than those at BATS (Figure 8b).

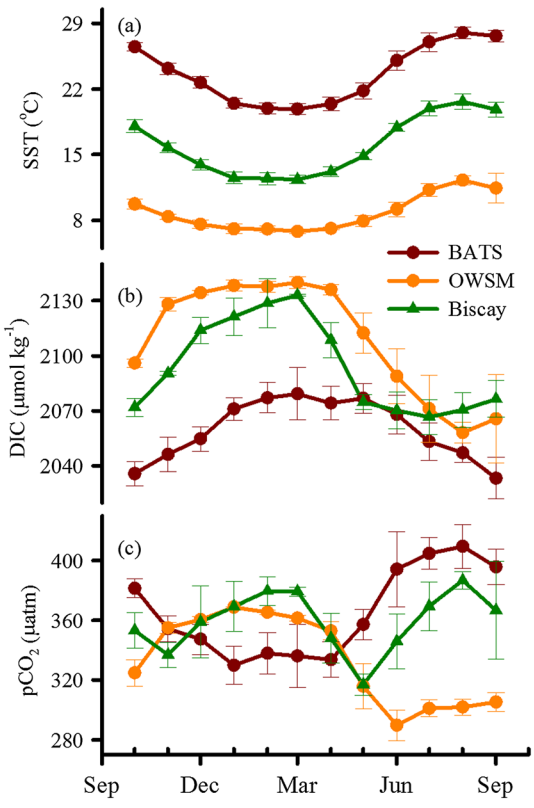

Figure 8. The seasonal variations of SST (a), DIC (b), and pCO_2 (c) in regions at different latitudes in the North Atlantic: BATS, OWSM, and Bay of Biscay. The available data during 2003–2010 are presented, and the error bars show the standard deviations of the monthly averaged values in different years.

[44] As shown in Figure 8c, the seasonal variation in pCO_2 has a different pattern at different latitudinal locations. In the oligotrophic subtropical gyre with low biological production rate (BATS and ESTOC), seawater pCO_2 is dominated by temperature with a single summer maximum and a single winter minimum [*Bates et al.*, 1996; *González-Dávila et al.*, 2003]. In contrast, in the high-latitude North Atlantic, it has generally been reported that changes in pCO_2 occur in parallel to those of DIC with a single-peak annual cycle, which is opposite to that in the oligotrophic subtropical gyre [*Körtzinger et al.*, 2008; *Olsen et al.*, 2008; *Takahashi et al.*, 1993].

[45] The Bay of Biscay is located in the transition region between the northern seasonally stratified subpolar gyre and the southern permanently stratified subtropical gyre [*McKinley et al.*, 2011]. The double-peak annual cycle of pCO_2 in the Bay of Biscay displayed a seasonal evolution between the DIC-dominated variability and the temperature-dominated variability (Figure 8c). As discussed in section 4.2, the pCO_2 variations in the Bay of Biscay followed the changes in DIC from autumn to spring, which was similar to that at OWSM. However, the winter upward supply of nutrients in the Bay of Biscay was lower than that at OWSM (Table 3), which resulted in an earlier nutrient depletion (started from May associated with surface stratification, Figure 2). During the post-bloom period, the nutrient-depleted and stratified condition in the Bay of Biscay was similar to that in the oligotrophic subtropical gyre. Therefore, the pCO_2 variability displayed a temperature-dominated pattern in summer months similar to the BATS (Figure 8c).

7. Interannual Variability of DIC, pCO_2, and Air-Sea CO_2 Flux

[46] The time series of carbon system observations in the Bay of Biscay can be extended back from 2010 to 2002 by including earlier observations [*Padin et al.*, 2008; *Dumousseaud et al.*, 2010]. The available data from 2002 to 2010 are shown in Figure 9, and the key points are summarized in Table 4. The evolutions of SST, MLD, DIC, and nutrients in the Bay of Biscay showed similar seasonal trends in all years in 2002–2010 as described in section 3. However, their seasonal amplitudes showed notable year-to-year variations, which were mainly due to the differences in winter conditions (Figure 9 and Table 4). The winter minima in SST ranged from 11.8 °C to 13.1 °C from 2002 to 2010. Higher winter SSTs were observed in the warmer winters of 2006/2007 and 2007/2008 when the surface air temperature was the warmest on record for 500 years [*Luterbacher et al.*, 2007]. The SST anomalies were related

Table 3. Comparison of the Seasonal Biogeochemical Variations of the Surface Water in the North Atlantic

Region/Site	Type	SST (°C)	Salinity	TA (umol kg^{-1})	MLD[e] (m)	DIC (μmol kg^{-1})	NO_x (μmol kg^{-1})	pCO_2 (μatm)
ESTOC[a]	variation range	18 to 24	36.6 to 37.0	2399 to 2424	25 to 200	~2085 to ~2105	ND[f] to 1.5	~320 to ~400
29°10′N, 15°30′W	seasonal amplitude	4 to 6	0.4	25		20 to 30	1.5	60 to 70
BATS[b]	variation range	19 to 28	36.2 to 36.9	2365 to 2405	10 to 250	2010 to 2065	ND to detectable	310 to 410
31°50′N, 64°10′W	seasonal amplitude	7 to 10	0.6	20 to 30		40 to 50		90 to 100
Bay of Biscay[c]	variation range	11.8 to 21.5	35.5 to 35.7	2336 to 2364	20 to 500	~2060 to ~2135 (cold winter)	ND to 7.9 (cold winter)	~320 to ~390
						~2060 to ~2110 (warm winter)	ND to 3.9 (warm winter)	
45–46.5°N, 4–6°W	seasonal amplitude	6.4 to 9.5	0.2	15 to 26		47 (warm winter) to 80 (cold winter)	3.9 (warm winter) to 7.9 (cold winter)	~50 to 75
OWSM[d]	variation range	6 to 14	34.8 to 35.2		20 to 300	~2040 to ~2140	ND to 12	~290 to ~370
66°N, 2°W	seasonal amplitude	5 to 8	0.4			~80 to ~100	~12	~80

[a] *González-Dávila et al.* [2003], *Santana-Casiano et al.* [2007].
[b] *Bates et al.* [1996], *Bates* [2001, 2007].
[c] *Padin et al.* [2008], *Dumousseaud et al.* [2010], and this study.
[d] *Skjelvan et al.* [2008].
[e] MLDs in different studies may be estimated from various criteria.
[f] ND: not detectable.

to the changes in oceanic convection: a regression analysis of winter minima in SST and maxima in MLD results in a negative correlation ($R^2 = 0.80$). In the warmer-than-average years, shallower winter MLDs were developed and decreased winter mixing results in lower wintertime concentrations and seasonal amplitudes of DIC and nutrients (Figure 9 and Table 4). Similar correlations between the winter anomalies of SST, MLD, and DIC have also been established in the North Atlantic subtropical gyre [*Bates*, 2007; *González-Dávila et al.*, 2007; *Gruber et al.*, 2002]. In contrast, in the North Atlantic subpolar gyre the largest differences in DIC between years have tended to be observed during summer [*Corbiere et al.*, 2007; *Findlay et al.*, 2008; *Skjelvan et al.*, 2008].

[47] In the Bay of Biscay, seasonal patterns of pCO_2 in 2008–2010 and 2002–2004 were similar: with high values observed later in winter and summer (Figure 9f). The seasonal ranges in 2008–2010 (75 and 61 μatm) were also similar to those in 2002–2004 (63 and 45 μatm). Compared to the simple correlation between variations of DIC and winter mixing, the interannual variability in seawater pCO_2 is more complicated due to the counteracting effects of temperature versus nonthermal processes. The net changes in pCO_2 depend on the balance of the opposing effects of changes in SST and DIC, which may cancel each other out. For example, higher SST in a warmer winter will support a higher pCO_2, but the decreased concentrations of DIC will lead to a lower pCO_2.

[48] An increase in annual averaged seawater $pCO_{2,sea}$ was found from 2002–2004 (340 ± 18 and 336 ± 14 μatm, annual mean ± standard deviation of the monthly values) to 2008–2010 (359 ± 22 and 369 ± 19 μatm). This rise of 20–30 μatm is considerably more rapid than the rate of increase in the atmosphere over the same time interval (~13 μatm estimated from measurements at land stations). In order to examine the changes in the annual air-sea CO_2 flux, we have applied an identical calculation method to all the data sets obtained between 2002 and 2010 in the Bay of Biscay. The annual flux estimated using the QuikSCAT wind data and the *Nightingale et al.* [2000] parameterization (Table 2) suggests that the capacity of CO_2 uptake of the Bay of Biscay has decreased from 2002–2004 (-1.47 and -1.68 mol m^{-2} yr^{-1}) to 2008–2010 (-0.97 and -0.75 mol m^{-2} yr^{-1}). These results are similar to those obtained in several other studies which also found reduced rates of ocean CO_2 uptake in the North Atlantic in recent years [*Corbiere et al.*, 2007; *Schuster et al.*, 2009; *Watson et al.*, 2009]. However, a study based on data from 1981 to 2009 [*McKinley et al.*, 2011] suggests that trends in oceanic CO_2 concentration converge with atmospheric trends over the 29-year period, overcoming the influence of variability on decadal scale.

8. Interannual Variability and Its Link With Large-Scale Climate Variations

[49] Understanding of the link between local interannual variability and large-scale climate patterns is thought to be critical for improving our knowledge of both the controls on natural ocean biogeochemistry and the potential impact of future climate change [*Bates*, 2007; *Corbiere et al.*, 2007]. The North Atlantic Oscillation (NAO) is the dominant mode of the atmospheric pressure variation over

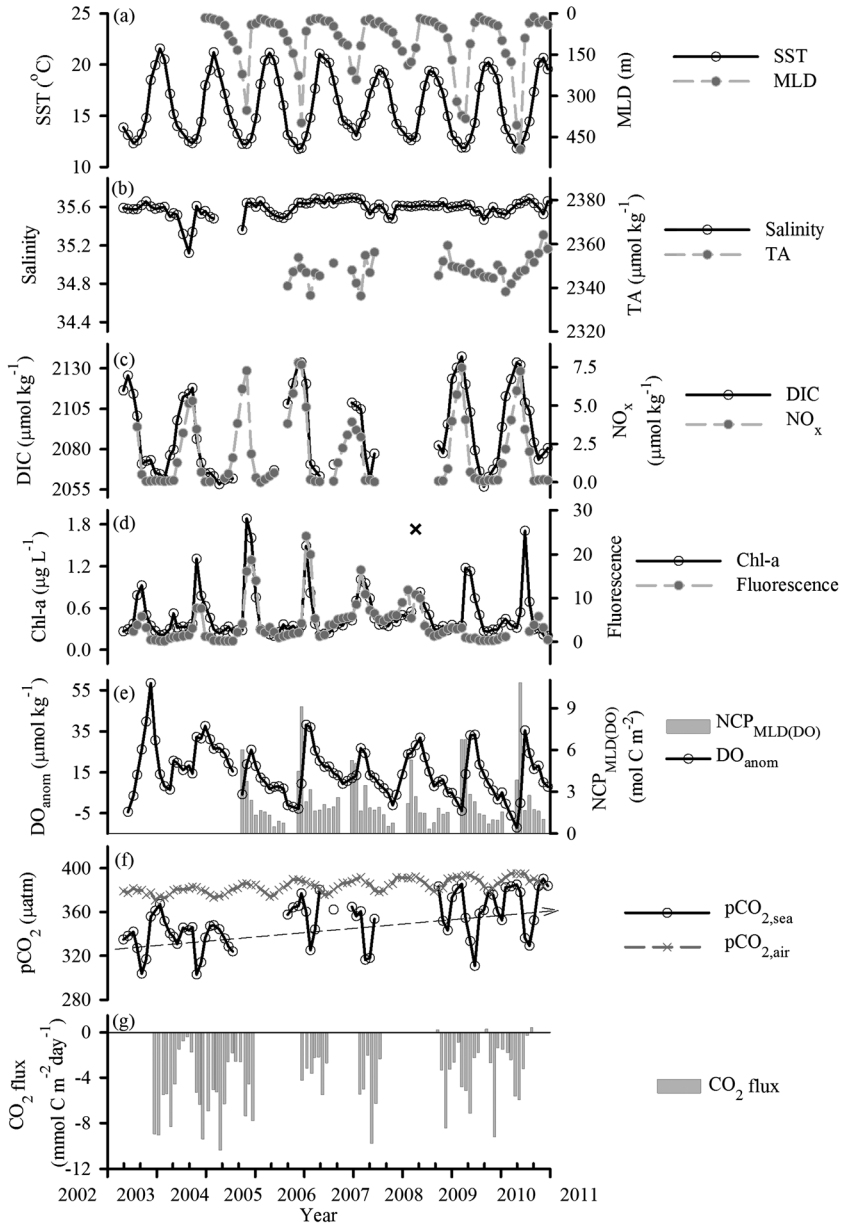

Figure 9. The interannual variability in the Bay of Biscay from 2002 to 2010: (a) SST and MLD; (b) salinity and TA; (c) DIC and NO_x; (d) remotely sensed Chl-*a* concentration and underway fluorescence; (e) DO_{anom} and mixed-layer integrated net community production (NCP_{MLD}); (f) atmospheric $pCO_{2,air}$ and seawater $pCO_{2,sea}$; (g) air-sea CO_2 flux. Comparison between the remotely sensed Chl-*a* concentration and the underway fluorescence suggested an outliner in the remotely sensed Chl-*a* in spring 2008, which was highlighted as a cross in Figure 9d.

the North Atlantic [*Marshall et al*., 2001; *Visbeck et al*., 2003]. In the western North Atlantic subtropical gyre, interannual variations of SST, MLD, DIC, and NCP appear to be correlated with the variability of NAO [*Bates*, 2001, 2007; *Gruber et al*., 2002]. *Gruber et al*. [2002] concluded that the carbon variability at BATS is largely driven by variations in winter SST and MLD linked to the NAO and suggested that the entire North Atlantic may vary in a basin-wide coordinated pattern. However, studies at ESTOC suggested that the oceanic response in the eastern North Atlantic subtropical gyre is apparently delayed by 3 years relative to the shifts in the NAO and was instead more directly related to the East Atlantic pattern (EA) [*González-Dávila et al*., 2003, 2007; *Santana-Casiano et al*., 2007].

[50] The NAO is most strongly expressed in the atmosphere in winter with a positive phase associated with positive SST anomalies and less vigorous winter mixing in the northern European marginal seas [*Cayan*, 1992; *Cullen et al*., 2001]. In the Bay of Biscay, *Padin et al*. [2008] suggested that the meteorological conditions during the formation of winter MLD have a significant influence on the biogeochemical behavior. Changes in MLD and hydrographic structure and their effect on the marine ecosystem and biogeochemistry in the southern Bay of Biscay have

Table 4. The Interannual Differences in the Bay of Biscay from 2003 to 2010 Including the Years 2006/2007 and 2007/2008 with Exceptionally Warm Winters

	Winter Condition					Annual Amplitude			Spring Bloom (February– May)		
Year	Mean NAO	Mean EA	Min SST (°C)	Max MLD (m)	Max NO_x (μmol kg^{-1})	Max DIC (μmol kg^{-1})	SST (°C)	NO_x (μmol kg^{-1})	DIC (μmol kg^{-1})	Integrated $NCP_{MLD(DO)}$ (mol C m^{-2})	Integrated CO_2 flux (mol C m^{-2})
2003/2004	0.31	0.15	12.34		5.30		9.07	5.27			
2004/2005	0.21	−0.99	12.25	348	7.25		8.90	7.27		13.83	
2005/2006	−0.24	−0.88	11.76	423	7.76	2133	9.29	7.73	70	16.94	−0.31
2006/2007	0.63	1.10	13.06	230	3.93	2109	7.64	3.91	47	13.36	−0.71
2007/2008	0.51	0.04	12.61	177			6.77			11.20	
2008/2009	0.09	−0.59	11.89	437	7.45	2137	8.36	7.41	81	15.83	−0.48
2009/2010	−1.48	0.95	11.81	496	7.22	2134	8.86	7.13	62	14.40	−0.39

been related to the atmospheric forcing [*Cabrillo et al*., 2011; *Somavilla et al*., 2009]. A reconstruction of MLD variability in the southern Bay of Biscay over the past 60 years suggested that decadal variability in MLD seems to follow the NAO, while the negative phase of EA may result in intense episodes of cooling and deep mixing [*Cabrillo et al*., 2011; *Somavilla et al*., 2009].

[51] As shown in Table 4, we examined the link between the wintertime indices of NAO and EA (averaged throughout December to March) and the biogeochemical variability in the Bay of Biscay. According to our analysis, the interannual variability of winter mixing is likely to be more affected by the NAO: the winter maximum MLD shows a negative correlation with the winter mean NAO index ($R^2 = 0.66$, $p = 0.05$), but its correlation with winter mean EA index is not significant ($R^2 = 0.04$, $p = 0.71$). Positive wintertime NAO index tends to coincide with shallower winter MLDs in the Bay of Biscay, especially in the 2006/2007 and 2007/2008 with warm winters. This is similar to that at BATS [*Bates*, 2001, 2007; *Gruber et al*., 2002] but is opposite to that in the subpolar gyre [*Carton et al*., 2008; *Henson et al*., 2009]. As shown in Table 4 and Figure 9, the warm winters and shallow winter MLDs corresponded to lower winter concentrations and seasonal amplitudes of DIC and NO_x, as well as reduced Chl-*a* concentrations and NCP_{MLD} in the following spring bloom. In contrast, higher seasonal ranges of DIC and NO_x were observed in cold years with deep winter mixing, which appear to be associated with the negative winter NAO indices.

[52] It is predicted that shallower winter MLDs in the future, under global warming, would result in a consequent reduction in primary production and oceanic CO_2 uptake in low and midlatitudinal oceans [*Bopp et al*., 2001; *Sarmiento et al*., 1998] as well as in the North Atlantic [*Gruber et al*., 2002]. However, our study in the Bay of Biscay has shown that a reduction in NCP associated with a shallow winter MLD does not necessarily result in a decrease in CO_2 uptake by the ocean. Following the reduced winter convection in 2006/2007, the NCP_{MLD} did indeed decrease during the bloom period, but the integrated CO_2 sink was nevertheless stronger than those in other years (Table 4). As discussed by *Dumousseaud et al*. [2010], this is mainly explained by a smaller amount of seasonal warming from winter to summer which resulted in a smaller pCO_2 rise, together with higher wind speeds which facilitated gas exchange.

9. Conclusions

[53] In the midlatitude Northeast Atlantic (Bay of Biscay), the seasonality of DIC is shaped by the winter increase due to deep convection followed by the spring biological drawdown. The stoichiometry of carbon and nutrient utilization did not show "carbon overconsumption" during the bloom period when nutrients were not limiting, but non-Redfield uptake was observed in the post-bloom summer with nutrient stress. Determined by the balance of the competing effect of temperature and nonthermal processes on pCO_2, the annual cycle of pCO_2 in the Bay of Biscay was characterized by a double-peak distribution. The temperature-dominated summer pCO_2 peak is similar to that in the North Atlantic subtropical gyre, while the winter pCO_2 peak following the DIC changes is similar to the observations in

subpolar North Atlantic. Similar to results at BATS in the western North Atlantic subtropical gyre, the interannual DIC variations in the Bay of Biscay were mainly modulated by the changes in the strength of winter mixing. The seasonal amplitudes of DIC and NO_x were higher in years with cold winters and deep MLDs, apparently in response to the negative phases of the NAO. The Bay of Biscay was overall an atmospheric CO_2 sink because of greater CO_2 uptake in autumn and spring compared to the states of equilibrium or slight CO_2 oversaturation in winter and summer. An increase in annual mean seawater pCO_2 was observed from 2002–2004 to 2008–2010 (340 and 336 μatm to 359 and 369 μatm) associated with decreased rates of oceanic CO_2 uptake (-1.47 and $-1.68\,mol\,m^{-2}\,yr^{-1}$ to -0.97 and $-0.75\,mol\,m^{-2}\,yr^{-1}$).

[54] **Acknowledgments.** This work was supported by the UK DEFRApH, the EU EPOCA projects, and the EU FP7 project CARBOCHANGE "Changes in carbon uptake and emissions by oceans in a changing climate" funded by the European Community's Seventh Framework Programme (no. 264879). Swire Education Trust is thanked for providing Zong-Pei Jiang's scholarship. We thank all the technicians and students who contributed to the POB project. We are grateful for the assistance of the P&O Ferries Ltd. and the captain and crews of *Pride of Bilbao*. Maureen Pagnani is thanked for the help on processing the MLD data. We thank three anonymous reviewers for their comments, which significantly improved the quality of this paper.

References

Abril, G., H. Etcheber, B. Delille, M. Frankignoulle, and A. V. Borges (2003), Carbonate dissolution in the turbid and eutrophic Loire estuary, *Mar. Ecol. Prog. Ser.*, *259*, 129–138, doi:10.3354/meps259129.

Abril, G., H. Etcheber, P. Le Hir, P. Bassoullet, B. Boutier, and M. Frankignoulle (1999), Oxic/anoxic oscillations and organic carbon mineralization in an estuarine maximum turbidity zone (The Gironde, France), *Limnol. Oceanogr.*, *44*(5), 1304–1315, doi:10.4319/lo.1999.44.5.1304.

Abril, G., M. V. Commarieu, D. Maro, M. Fontugne, F. Guerin, and H. Etcheber (2004), A massive dissolved inorganic carbon release at spring tide in a highly turbid estuary, *Geophys. Res. Lett.*, *31*(9), doi:10.1029/2004gl019714.

Bargeron, C. P., D. J. Hydes, D. K. Woolf, B. A. Kelly-Gerreyn, and M. A. Qurban (2006), A regional analysis of new production on the northwest European shelf using oxygen fluxes and a ship-of-opportunity, *Estuarine, Coastal Shelf Sci.*, *69*(3-4), 478–490, doi:10.1016/j.ecss.2006.05.015.

Bates, N. R. (2001), Interannual variability of oceanic CO_2 and biogeochemical properties in the Western North Atlantic subtropical gyre, *Deep Sea Res., Part II*, *48*(8-9), 1507–1528, doi:10.1016/S0967-0645(00)00151-X.

Bates, N. R. (2007), Interannual variability of the oceanic CO_2 sink in the subtropical gyre of the North Atlantic Ocean over the last 2 decades, *J. Geophys. Res.*, *112*(C9), C09013, doi:10.1029/2006jc003759.

Bates, N. R., A. F. Michaels, and A. H. Knap (1996), Seasonal and interannual variability of oceanic carbon dioxide species at the U.S. JGOFS Bermuda Atlantic Time-series Study (BATS) site, *Deep Sea Res., Part II*, *43*(2-3), 347–383, doi:10.1016/0967-0645(95)00093-3.

Benson, B. B., and D. Krause (1984), The concentration and isotopic fractionation of oxygen dissolved in fresh-water and seawater in equilibrium with the atmosphere, *Limnol. Oceanogr.*, *29*(3), 620–632, doi:10.4319/lo.1984.29.3.0620.

Bopp, L., P. Monfray, O. Aumont, J. L. Dufresne, H. Le Treut, G. Madec, L. Terray, and J. C. Orr (2001), Potential impact of climate change on marine export production, *Global Biogeochem. Cycles*, *15*(1), 81–99, doi:10.1029/1999 GB001256.

Bozec, Y., H. Thomas, L. S. Schiettecatte, A. V. Borges, K. Elkalay, and H. J. W. de Baar (2006), Assessment of the processes controlling seasonal variations of dissolved inorganic carbon in the North Sea, *Limnol. Oceanogr.*, *51*(6), 2746–2762, doi:10.4319/lo.2006.51.6.2746.

Cabrillo, R. S., C. Gonzalez-Pola, M. Ruiz-Villarreal, and A. L. Montero (2011), Mixed layer depth (MLD) variability in the southern Bay of Biscay. Deepening of winter MLDs concurrent with generalized upper water warming trends?, *Ocean Dynam.*, *61*(9), 1215–1235, doi:10.1007/s10236-011-0407-6.

Cai, W. J., X. P. Hu, W. J. Huang, L. Q. Jiang, Y. C. Wang, T. H. Peng, and X. Zhang (2010), Alkalinity distribution in the western North Atlantic Ocean margins, *J. Geophys. Res.*, *115*, C08014, doi:10.1029/2009jc005482.

Carton, J. A., S. A. Grodsky, and H. Liu (2008), Variability of the oceanic mixed layer, 1960-2004, *J. Clim.*, *21*(5), 1029–1047, doi:10.1175/2007jcli1798.1.

Cayan, D. R. (1992), Latent and sensible heat-flux anomalies over the Northern Oceans—driving the sea-surface temperature, *J. Phys. Oceanogr.*, *22*(8), 859–881, doi:10.1175/1520-0485(1992)022 < 0859:LASHFA > 2.0.CO;2.

Chou, W.-C., Y.-L. L. Chen, D. D. Sheu, Y.-Y. Shih, C.-A. Han, C. L. Cho, C.-M. Tseng, and Y.-J. Yang (2006), Estimated net community production during the summertime at the SEATS time-series study site, northern South China Sea: Implications for nitrogen fixation, *Geophys. Res. Lett.*, *33*(22), L22610, doi:10.1029/2005gl025365.

Corbiere, A., N. Metzl, G. Reverdin, C. Brunet, and A. Takahashi (2007), Interannual and decadal variability of the oceanic carbon sink in the North Atlantic subpolar gyre, *Tellus, Ser. B*, *59*(2), 168–178, doi:10.1111/j.1600-0889.2006.00232.x.

Cullen, H. M., R. D. D'Arrigo, E. R. Cook, and M. E. Mann (2001), Multiproxy reconstructions of the North Atlantic Oscillation, *Paleoceanography*, *16*(1), 27–39, doi:10.1029/1999PA000434.

Dickson, A. G. (1990), Standard potential of the $(AgCl(s) + ½\,H_2(g) = Ag(s) + HCl(aq))$ cell and the dissociation constant of bisulfate ion in synthetic sea water from 273.15 to 318.15 K, *J. Chem. Thermodyn.*, *22*, 113–127, doi:10.1016/0021-9614(90)90074-Z.

Dickson, A. G., and F. J. Millero (1987), A comparison of the equilibrium constants for the dissociation of carbonic acid in the seawater media, *Deep Sea Res.*, *34*, 1733–1743, doi:10.1016/0198-0149(87)90021-5.

Dickson, A. G., C. L. Sabine, and J. R. Christian (2007), Guide to best practices for ocean CO_2 measurements, 191 pp., PICES Special Publication 3, Sidney, British Columbia.

Dumousseaud, C., E. P. Achterberg, T. Tyrrell, A. Charalampopoulou, U. Schuster, M. Hartman, and D. J. Hydes (2010), Contrasting effects of temperature and winter mixing on the seasonal and interannual variability of the carbonate system in the Northeast Atlantic Ocean, *Biogeosciences*, *7*(5), 1481–1492, doi:10.5194/bg-7-1481-2010.

Feely, R. A., C. L. Sabine, J. M. Hernandez-Ayon, D. Ianson, and B. Hales (2008), Evidence for upwelling of corrosive "acidified" water onto the continental shelf, *Science*, *320*(5882), 1490–1492, doi:10.1126/science.1155676.

Findlay, H. S., T. Tyrrell, R. G. J. Bellerby, A. Merico, and I. Skjelvan (2008), Carbon and nutrient mixed layer dynamics in the Norwegian Sea, *Biogeosciences*, *5*(5), 1395–1410, doi:10.5194/bg-5-1395-2008.

Friis, K., A. Kortzinger, and D. W. R. Wallace (2003), The salinity normalization of marine inorganic carbon chemistry data, *Geophys. Res. Lett.*, *30*(2), 1085, doi:10.1029/2002gl015898.

Fung, I. Y., S. C. Doney, K. Lindsay, and J. John (2005), Evolution of carbon sinks in a changing climate, *Proc. Natl. Acad. Sci. U. S. A.*, *102*(32), 11201–11206, doi:10.1073/pnas.0504949102.

Gattuso, J.-P., and L. Hansson (Eds.) (2011), *Ocean Acidification*, 352 pp., Oxford University Press, Oxford.

González-Dávila, M., J. M. Santana-Casiano, and E. F. González-Dávila (2007), Interannual variability of the upper ocean carbon cycle in the northeast Atlantic Ocean, *Geophys. Res. Lett.*, *34*(7), L07608, doi:10.1029/2006gl028145.

González-Dávila, M., J. M. Santana-Casiano, M. J. Rueda, O. Llinas, and E. F. Gonzalez-Davila (2003), Seasonal and interannual variability of sea-surface carbon dioxide species at the European Station for Time Series in the Ocean at the Canary Islands (ESTOC) between 1996 and 2000, *Global Biogeochem. Cycles*, *17*(3), 1076, doi:10.1029/2002gb001993.

González-Pola, C., J. M. Fernández-Díaz, and A. Lavín (2007), Vertical structure of the upper ocean from profiles fitted to physically consistent functional forms, *Deep Sea Res., Part I*, *54*(11), 1985–2004, doi:10.1016/j.dsr.2007.08.007.

Gruber, N., C. D. Keeling, and N. R. Bates (2002), Interannual variability in the North Atlantic Ocean carbon sink, *Science*, *298*(5602), 2374–2378, doi:10.1126/science.1077077.

Hansen, H. P., and F. Koroleff (2007), Determination of nutrients, in *Methods of Seawater Analysis*, edited by K. Grasshoff, M. Ehrhardt and K. Kremling, pp. 159–228, Wiley-VCH Verlag GmbH, Weinheim, Germany.

Henson, S. A., J. P. Dunne, and J. L. Sarmiento (2009), Decadal variability in North Atlantic phytoplankton blooms, *J. Geophys. Res.*, *114*, C04013, doi:10.1029/2008jc005139.

Hoffman, R. N. (2011), Neutral stability height correction for ocean winds, *arXiv:1107.1416v1 [physics.ao-ph]*.

Hydes, D. J., M. C. Hartman, J. Kaiser, and J. M. Campbell (2009), Measurement of dissolved oxygen using optodes in a FerryBox system, *Estuarine, Coastal Shelf Sci.*, *83*(4), 485–490, doi:10.1016/j.ecss.2009.04.014.

Hydes, D. J., R. J. Gowen, N. P. Holliday, T. Shammon, and D. Mills (2004), External and internal control of winter concentrations of nutrients (N, P and Si) in north-west European shelf seas, *Estuar. Coast. Shelf Sci.*, *59*(1), 151–161, doi:10.1016/j.ecss.2003.08.004.

Hydes, D. J., et al. (2003), Use of a Ferry-Box system to look at shelf sea and ocean margin processes, in *Elsevier Oceanography Series*, edited by H. Dahlin, N. C. Flemming, K. Nittis and S. E. Petersson, pp. 297–303, Elsevier, Athens, Greece.

Johnson, K. S., S. C. Riser, and D. M. Karl (2010), Nitrate supply from deep to near-surface waters of the North Pacific subtropical gyre, *Nature*, *465* (7301), 1062–1065, doi:10.1038/Nature09170.

Kelly-Gerreyn, B. A., D. J. Hydes, A. M. Jégou, P. Lazure, L. J. Fernand, I. Puillat, and C. Garcia-Soto (2006), Low salinity intrusions in the western English Channel, *Cont. Shelf Res.*, *26*(11), 1241–1257, doi:10.1016/j.csr.2006.03.007.

Klausmeier, C. A., E. Litchman, T. Daufresne, and S. A. Levin (2004), Optimal nitrogen-to-phosphorus stoichiometry of phytoplankton, *Nature*, *429*(6988), 171–174, doi:10.1038/Nature02454.

Koeve, W. (2004), Spring bloom carbon to nitrogen ratio of net community production in the temperate N. Atlantic, *Deep Sea Res., Part I*, *51*(11), 1579–1600, doi:10.1016/j.dsr.2004.07.002.

Koeve, W. (2006), C: N stoichiometry of the biological pump in the North Atlantic: Constraints from climatological data, *Global Biogeochem. Cycles*, *20*(3), GB3018, doi:10.1029/2004gb002407.

Körtzinger, A., W. Koeve, P. Kahler, and L. Mintrop (2001), C: N ratios in the mixed layer during the productive season in the northeast Atlantic Ocean, *Deep Sea Res., Part I*, *48*(3), 661–688, doi:10.1016/S0967-0637(00)00051-0.

Körtzinger, A., U. Send, R. S. Lampitt, S. Hartman, D. W. R. Wallace, J. Karstensen, M. G. Villagarcia, O. Llinás, and M. D. DeGrandpre (2008), The seasonal pCO_2 cycle at 49°N/16.5°W in the northeastern Atlantic Ocean and what it tells us about biological productivity, *J. Geophys. Res.*, *113*(C4), C04020, doi:10.1029/2007jc004347.

Lavin, A., L. Valdes, F. Sanchez, P. Abaunza, A. Forest, B. Boucher, P. Lazure, and A. M. Jegou (2006), The Bay of Biscay: the encountering of the ocean and the shelf, in *The Sea* edited by A. R. Robinson and K. H. Brink, pp. 933–1001, Harvard University Press, Harvard.

Le Quere, C., et al. (2009), Trends in the sources and sinks of carbon dioxide, *Nat. Geosci.*, *2*(12), 831–836, doi:10.1038/Ngeo689.

Lee, K., L. T. Tong, F. J. Millero, C. L. Sabine, A. G. Dickson, C. Goyet, G. H. Park, R. Wanninkhof, R. A. Feely, and R. M. Key (2006), Global relationships of total alkalinity with salinity and temperature in surface waters of the world's oceans, *Geophys. Res. Lett.*, *33*(19), L19605, doi:10.1029/2006gl027207.

Lewis, E., and D. Wallace (1998), Program Developed for CO_2 System Calculations.

Luterbacher, J., M. A. Liniger, A. Menzel, N. Estrella, P. M. Della-Marta, C. Pfister, T. Rutishauser, and E. Xoplaki (2007), Exceptional European warmth of autumn 2006 and winter 2007: Historical context, the underlying dynamics, and its phenological impacts, *Geophys. Res. Lett.*, *34*(12), L12704, doi:10.1029/2007gl029951.

Marshall, J., H. Johnson, and J. Goodman (2001), A study of the interaction of the North Atlantic oscillation with ocean circulation, *J. Clim.*, *14*(7), 1399–1421, doi:10.1175/1520-0442(2001)014 < 1399:ASOTIO > 2.0.CO;2.

McGillis, W. R., J. B. Edson, J. D. Ware, J. W. H. Dacey, J. E. Hare, C. W. Fairall, and R. Wanninkhof (2001), Carbon dioxide flux techniques performed during GasEx-98, *Mar. Chem.*, *75*(4), 267–280, doi:10.1016/S0304-4203(01)00042-1.

McKinley, G. A., A. R. Fay, T. Takahashi, and N. Metzl (2011), Convergence of atmospheric and North Atlantic carbon dioxide trends on multi-decadal time scales, *Nat. Geosci.*, *4*(9), 606–610, doi:10.1038/Ngeo1193.

Mehrbach, C., C. H. Culberson, J. E. Hawley, and R. M. Pytkowicz (1973), Measurement of the apparent dissociation constants of carbonic acid in seawater at atmospheric pressure, *Limnol. Oceanogr.*, *18*, 897–907, doi:10.4319/lo.1973.18.6.0897.

Nightingale, P. D., G. Malin, C. S. Law, A. J. Watson, P. S. Liss, M. I. Liddicoat, J. Boutin, and R. C. Upstill-Goddard (2000), In situ evaluation of air-sea gas exchange parameterizations using novel conservative and volatile tracers, *Global Biogeochem. Cycles*, *14*(1), 373–387, doi:10.1029/1999 GB900091.

Olsen, A., K. R. Brown, M. Chierici, T. Johannessen, and C. Neill (2008), Sea-surface CO_2 fugacity in the subpolar North Atlantic, *Biogeosciences*, *5*(2), 535–547, doi:10.5194/bg-5-535-2008.

Orr, J. C., et al. (2005), Anthropogenic ocean acidification over the twenty-first century and its impact on calcifying organisms, *Nature*, *437*(7059), 681–686, doi:10.1038/Nature04095.

Padin, X. A., C. G. Castro, A. F. Rios, and F. F. Perez (2008), fCO_2^{SW} variability in the Bay of Biscay during ECO cruises, *Cont. Shelf Res.*, *28*(7), 904–914, doi:10.1016/j.csr.2008.01.004.

Padin, X. A., G. Navarro, M. Gilcoto, A. F. Rios, and F. F. Perez (2009), Estimation of air-sea CO_2 fluxes in the Bay of Biscay based on empirical relationships and remotely sensed observations, *J. Mar. Syst.*, *75*(1-2), 280–289, doi:10.1016/j.jmarsys.2008.10.008.

Pollard, R. T., M. J. Griffiths, S. A. Cunningham, J. F. Read, F. F. Perez, and A. F. Rios (1996), Vivaldi 1991-A study of the formation, circulation and ventilation of Eastern North Atlantic Central Water, *Prog. Oceanogr.*, *37*(2), 167–192, doi:10.1016/S0079-6611(96)00008-0.

Quigg, A., Z. V. Finkel, A. J. Irwin, Y. Rosenthal, T. Y. Ho, J. R. Reinfelder, O. Schofield, F. M. M. Morel, and P. G. Falkowski (2003), The evolutionary inheritance of elemental stoichiometry in marine phytoplankton, *Nature*, *425*(6955), 291–294, doi:10.1038/Nature01953.

Redfield, A. C., B. H. Ketchum, and F. A. Richards (1934), On the proportions of organic derivatives in sea water and their relation to the composition of plankton in *James Johnstone Memorial Volume*, edited by R. J. Daniel, pp. 176–192, University Press of Liverpool, Liverpool.

Rees, A. P., J. A. Gilbert, and B. A. Kelly-Gerreyn (2009), Nitrogen fixation in the western English Channel (NE Atlantic Ocean), *Mar. Ecol. Prog. Ser.*, *374*, 7–12, doi:10.3354/meps07771.

Sabine, C. L., et al. (2004), The oceanic sink for anthropogenic CO_2, *Science*, *305*(5682), 367–371, doi:10.1126/science.1097403.

Sambrotto, R. N., G. Savidge, C. Robinson, P. Boyd, T. Takahashi, D. M. Karl, C. Langdon, D. Chipman, J. Marra, and L. Codispoti (1993), Elevated consumption of carbon relative to nitrogen in the surface ocean, *Nature*, *363*(6426), 248–250, doi:10.1038/363248a0.

Santana-Casiano, J. M., M. Gonzalez-Davila, M. J. Rueda, O. Llinas, and E. F. Gonzalez-Davila (2007), The interannual variability of oceanic CO_2 parameters in the northeast Atlantic subtropical gyre at the ESTOC site, *Global Biogeochem. Cycles*, *21*(1), C09013, doi:10.1029/2006gb002788.

Sarmiento, J. L., T. M. C. Hughes, R. J. Stouffer, and S. Manabe (1998), Simulated response of the ocean carbon cycle to anthropogenic climate warming, *Nature*, *393*(6682), 245–249, doi:10.1038/30455.

Schuster, U., A. J. Watson, N. R. Bates, A. Corbiere, M. Gonzalez-Davila, N. Metzl, D. Pierrot, and M. Santana-Casiano (2009), Trends in North Atlantic sea-surface fCO_2 from 1990 to 2006, *Deep Sea Res., Part II*, *56*(8-10), 620–629, doi:10.1016/j.dsr2.2008.12.011.

Skjelvan, I., E. Falck, F. Rey, and S. B. Kringstad (2008), Inorganic carbon time series at Ocean Weather Station M in the Norwegian Sea, *Biogeosciences*, *5*(2), 549–560, doi:10.5194/bg-5-549-2008.

Smith, H. E. K., et al. (2012), Predominance of heavily calcified coccolithophores at low $CaCO_3$ saturation during winter in the Bay of Biscay, *Proc. Natl. Acad. Sci. U. S. A.*, *109*(23), 8845–8849, doi:10.1073/pnas.1117508109.

Somavilla, R., C. Gonzalez-Pola, C. Rodriguez, S. A. Josey, R. F. Sanchez, and A. Lavin (2009), Large changes in the hydrographic structure of the Bay of Biscay after the extreme mixing of winter 2005, *J. Geophys. Res.*, *114*(C1), C01001, doi:10.1029/2008jc004974.

Sweeney, C., E. Gloor, A. R. Jacobson, R. M. Key, G. McKinley, J. L. Sarmiento, and R. Wanninkhof (2007), Constraining global air-sea gas exchange for CO_2 with recent bomb ^{14}C measurements, *Global Biogeochem. Cycles*, *21*(2), GB2015, doi:10.1029/2006gb002784.

Takahashi, T., J. Olafsson, J. G. Goddard, D. W. Chipman, and S C. Sutherland (1993), Seasonal variation of CO_2 and nutrients in the high-latitude surface ocean: a comparative study, *Global Biogeochem. Cycles*, *7*, 843–878, doi:10.1029/93 GB02263.

Takahashi, T., et al. (2009), Climatological mean and decadal change in surface ocean pCO_2, and net sea-air CO_2 flux over the global oceans, *Deep Sea Res., Part II*, *56*(8-10), 554–577, doi:10.1016/j.dsr2.2008.12.009.

Taylor, J. R. (1982), *An introduction to error analysis: The study of uncertainties in physical measurements*, 327 pp., University Science Books, Sausalito, Calif.

Toggweiler, J. R. (1993), Carbon overconsumption, *Nature*, *363*(6426), 210–211, doi:10.1038/363210a0.

Tyrrell, T. (2011), Anthropogenic modification of the oceans, *Philos. Trans. R. Soc., A*, *369*(1938), 887–908, doi:10.1098/rsta.2010.0334.

Visbeck, M., E. P. Chassignet, R. G. Curry, T. L. Delworth, R. R. Dickson, and G. Krahmann (2003), The ocean's response to North Atlantic Oscillation variability, in *The North Atlantic Oscillation: Climatic Significance and Environmental Impact*, edited by J. W. Hurrell, Y. Kushnir, G. Ottersen and M. Visbeck, pp. 113–145, AGU, Washington, DC.

Wanninkhof, R. (1992), Relationship between Wind-Speed and Gas-Exchange over the Ocean, *J. Geophys. Res.*, *97*(C5), 7373–7382, doi:10.1029/92JC00188.

Watson, A. J., et al. (2009), Tracking the variable North Atlantic sink for atmospheric CO_2, *Science*, *326*(5958), 1391–1393, doi:10.1126/science.1177394.

Weiss, R. F. (1974), Carbon dioxide in water and seawater: the solubility of a non-ideal gas, *Mar. Chem.*, *2*, 203–215, doi:10.1016/0304-4203(74)90015-2.

Wolf-Gladrow, D. A., R. E. Zeebe, C. Klaas, A. Kortzinger, and A. G. Dickson (2007), Total alkalinity: The explicit conservative expression and its application to biogeochemical processes, *Mar. Chem.*, *106*(1-2), 287–300, doi:10.1016/j.marchem.2007.01.006.